

Notes

Theoretical Study of the Reactions of Ethylene Oxide and Ammonia. A Model Study of the Epoxy Adhesive Curing Mechanism

Joseph W. Holubka*

Ford Motor Company, Dearborn, Michigan 48121

Robert D. Bach* and José L. Andrés

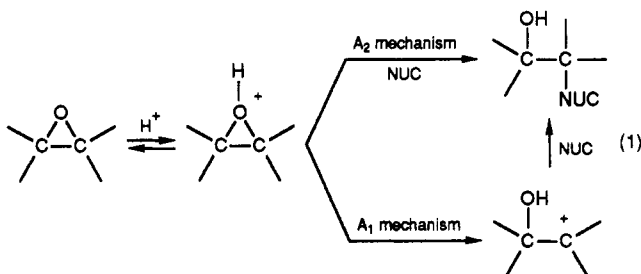
Department of Chemistry, Wayne State University,
Detroit, Michigan 48202

Received July 31, 1991

Revised Manuscript Received October 15, 1991

Introduction

The oxirane functional group undergoes a variety of addition reactions, and its enhanced reactivity is primarily a function of relief of ring strain. For example, the amination of epoxides is a useful synthetic method for the preparation of β -hydroxyamines.¹ However, the acidity of amines is generally insufficient for the reaction to proceed in the absence of a catalyst (e.g., BF_3). Hydrolysis or alcoholysis of epoxides in a preparative manner also requires a strong acid catalyst.² In aqueous media, the accepted protocol for oxirane cleavage is rapid reversible protonation with rate-determining ring opening (eq 1).³ For relatively unhindered systems, the trans stereospecificity and lack of carbenium ion rearrangements suggest a direct nucleophilic displacement (A_2 mechanism).³



The above fundamental reactions are germane to the mechanism of the curing process for structural adhesives and epoxy-based coatings that involve oxirane cleavage. It is generally accepted that the first step of this curing process involves a condensation reaction between an amine N-H functionality and an oxirane in a nucleophilic displacement that results in the formation of an alkanolamine. The rate of this reaction is sensitive to both the nature of the amine cross-linking agent and the solvent and is highly subject to catalysis. Thus, any mechanistic rationale concerning the reactivity of oxirane-terminated prepolymers must also include the location of the oxirane functionality in the molecule and its immediate molecular environment (i.e., solvents, catalysts, etc.). Within the context of epoxy resins used for either adhesives or coating cures, rate acceleration of the cross-linking process catalyzed by hydroxy functional groups is an integral part of the cure response time. An earlier explanation for this rate acceleration by the hydroxy functionality was pro-

posed by Schechter.⁴ It was suggested that polarization of the epoxide ring, which resulted from association of hydroxyl-containing compounds with the oxirane oxygen, lowered the barrier for ring cleavage. However, this is a concerted termolecular mechanism where the hydroxy functional group is required to hydrogen bond to the oxirane oxygen in the transition state.

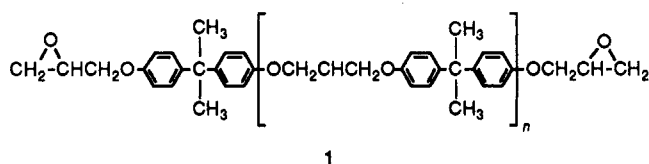
Subsequent mechanisms that have been suggested⁵⁻⁸ invoke bimolecular kinetics where the rate-determining step is a displacement by the nucleophilic amine on an epoxide-alcohol complex that is formed in a preequilibrium step (Scheme I).

Another mechanism that has been proposed⁹ explicitly considers the relative basicity of the amine and oxirane functionality. This overall process is similar to that in Scheme I except that it includes an equilibrium process between the amine and the proton donor that occurs prior to addition to the epoxide.

A convenient method to determine the sensitivity of the epoxy cure reactions to formulation variations involves the determination of gel times. In this procedure,¹⁰ the gel time is taken to be the time required from initial mixing to the formation of a continuous skin over a sample of cross-linking epoxy material. A range of gel times has been reported,¹⁰ for epoxy formulations with a series of hydroxy functional additives (Table I).

In general the gel time data establish a trend where the additives with increasing acidity effect the greatest increase in oxirane reactivity.¹⁰ With most protic additives, except carboxylic acids, there is nearly a linear relationship between the acidity of the additive and the reduction in gel time. Additional experimental data suggest that phenol accelerates the epoxy cure reaction more efficiently than aliphatic alcohols of lower acidity. The rate of oxirane cleavage is also seen (Table I) to increase as the functionality of the hydroxy-containing material is increased. This can be seen by a comparison of the gel times observed for reactions accelerated with trimethylolpropane versus propylene glycol and methanol.

The structure of the epoxy resin also influences the reactivity of the epoxy cure reaction. Most of the epoxy resins used in structural adhesives and coatings are of the Bisphenol A type having the general structure 1. Exper-



iments have shown that the reactivity is increased with increasing values of n . Control experiments have shown that the reactivity enhancement does not result from the presence of a residual phenolic functionality (i.e., from Bisphenol A) or epichlorohydrin that are the reactants used to prepare the epoxy resin. Instead data plotting the hydroxy content of the resin versus the epoxy equivalent weight of the resin shows a linear relationship that suggests that the enhancement in reactivity is the result of the

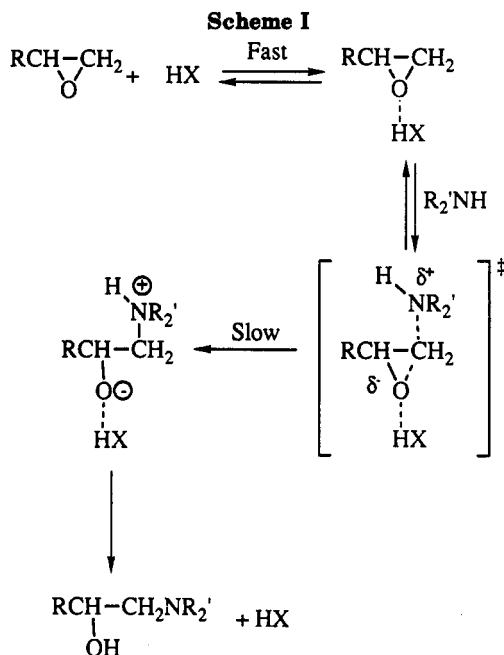


Table I
Effect of Additives on Gel Time

additive	decrease in gel time, min	additive	decrease in gel time, min
methanol	1	<i>o</i> -chlorophenol	15
butyl alcohol	2	<i>p</i> -nitrophenol	21
propylene glycol	8	acetic acid	12
trimethylolpropane	12	formic acid	18
phenol	13		

overall higher hydroxy content in the higher homologues of the epoxy resins.

In the present study we have three primary objectives. We would like to provide theoretical evidence based upon *ab initio* molecular orbital calculations that corroborates the general trend noted for the catalytic effect of proton donors on the curing rate of epoxy-based polymers. We will quantitatively describe the barriers for amination of ethylene oxide in the absence of catalysis, when it is fully protonated at oxirane oxygen and when it is hydrogen bonded to a molecule of water.

Results and Discussion

Molecular orbital calculations were carried out using the GAUSSIAN 88^{11a} program system utilizing gradient geometry optimization.^{11b} Preliminary geometry optimizations utilized the 3-21G basis set, and final geometry optimizations were carried out at the HF/6-31G* level. The geometry of the anti transition structures was constrained to be planar with O-C-C-N dihedral angles of 180°. A full set of vibrational frequencies were calculated for all four transition structures using analytical second derivatives. Only one imaginary frequency was found for each structure at the HF/6-31G* level. These first-order saddle points are therefore real transition states, and their structures are given in Figures 1-3.

Our first objective was to set a threshold barrier for oxirane cleavage by ammonia in the absence of a proton donor. The relative potential barriers for both syn and anti amination of ethylene oxide will also provide an assessment of the adverse electronic effects typically associated with a front-side S_N2 displacement. The anti ring-opening transition state (TS-2) of ethylene oxide by ammonia exhibited a barrier of 50.1 kcal/mol with the HF/6-31G* basis set. As anticipated, the front-side

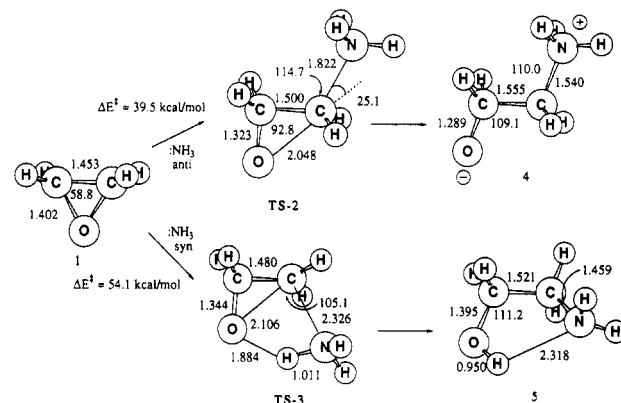


Figure 1. Calculated geometries of reactants, transition states, and products (HF/6-31G*) for anti (TS-2) and syn (TS-3) nucleophilic attack of ammonia on ethylene oxide. Energies are MP4SDTQ/6-31G*//HF/6-31G*.

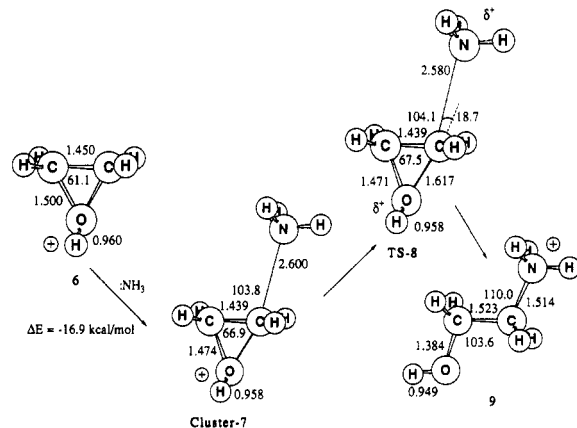


Figure 2. Calculated geometries of the reactant cluster, transition state, and product (HF/6-31G*) for the anti (TS-8) nucleophilic attack of ammonia on protonated ethylene oxide.

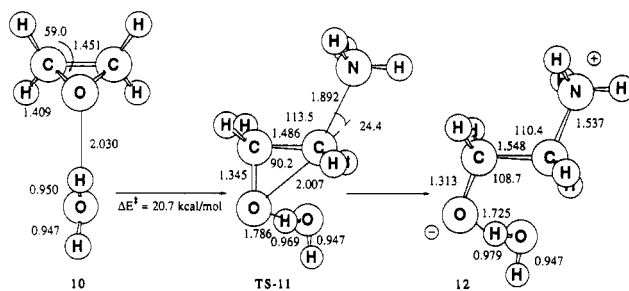


Figure 3. Calculated geometries of ethylene oxide complexed to water (10) and the transition state for the anti (TS-11) nucleophilic attack by ammonia (HF/6-31G*).

approach (TS-3) had a much higher barrier (66.4 kcal/mol) despite the potential for stabilization of the developing oxy anion by hydrogen bonding to the syn N-H bond (Figure 1). Møller-Plesset electron correlation correction to full fourth order (MP4SDTQ/6-31G*//HF/6-31G*) gave much lower barriers for TS-2 and TS-3 of 39.5 and 54.1 kcal/mol, respectively (Table II). This is a significant correction to the HF barrier, and consequently this MP4 correlation correction will be applied throughout the remainder of this paper.

As one might expect, in the absence of solvation, the trans amination affording zwitterionic product 4 is endothermic by 40.8 kcal/mol while syn ring opening giving the normal covalent hydrogen-bonded 2-aminoethanol (5) is attended by the liberation of 28.9 kcal/mol of energy. The heavy atoms in 4 were constrained to be anti periplanar, and no effort was made to find the global minimum

Table II
HF/6-31G* and MP4SDTQ/6-31G* Total Energies (in au) for the Optimized Geometries (Figure 1)* and Potential Barriers, ΔE^* , and Energy Differences, ΔE , between Isolated Reactants and Clusters or Final Products (in kcal/mol)

geometry	HF/6-31G*	MP4SDTQ/6-31G*	$\Delta E^*(\text{HF}/6-31\text{G}^*)$	$\Delta E^*(\text{MP4SDTQ}/6-31\text{G}^*)/\text{HF}/6-31\text{G}^*$	$\Delta E(\text{HF}/6-31\text{G}^*)$	$\Delta E(\text{MP4SDTQ}/6-31\text{G}^*)/\text{HF}/6-31\text{G}^*$
1	-152.867 356	-153.338 880				
TS-2	-208.971 805	-209.646 411	50.1	39.5		
TS-3	-208.945 888	-209.623 193	66.4	54.1		
4	-208.979 125	-209.644 370			45.5	40.8
5	-209.099 279	-209.755 439			-29.8	-28.9
6	-153.176 638	-153.642 484				
Cluster-7	-209.384 760	-210.039 470			-14.9	-16.6
TS-8	-209.384 720	-210.039 790	-14.9	-16.8		
9	-209.458 189	-210.096 479			-61.0	-52.4
10	-228.887 260	-229.557 805			-5.7	-7.9
TS-11	-285.007 725	-285.882 703	34.3	20.7		
12	-285.019 980	-285.885 289			26.7	19.1

* The total energies of ammonia and water at the two levels of theory are

	HF/6-31G*	MP4SDTQ/6-31G*//HF/6-31G*
ammonia	56.184 356	-56.370 495
water	-76.010 747	-76.206 321

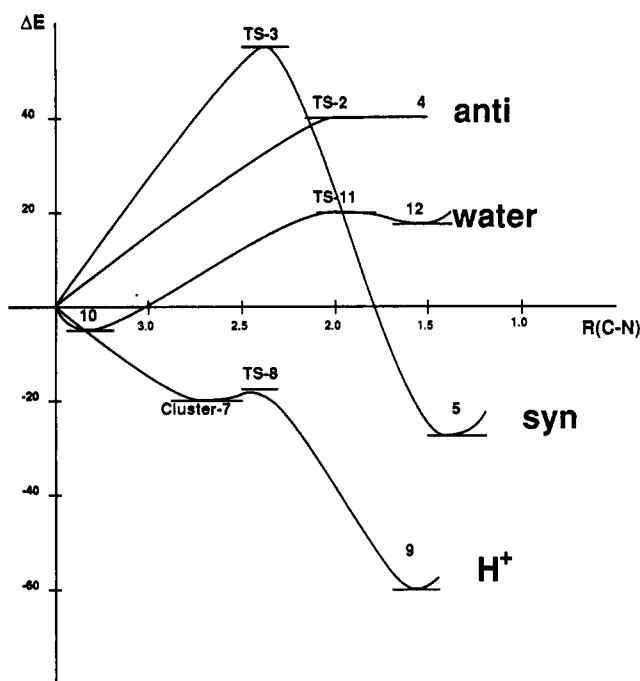


Figure 4. Potential energy profiles for the syn and anti nucleophilic attack of ammonia on ethylene oxide, protonated ethylene oxide, and ethylene oxide complexed with a water molecule. The energies are defined with respect to the isolated reactants and are given in kilocalories per mole. The C-N bond distance in angstroms is used as the reaction coordinate.

since C-C bond rotation and proton transfer would afford ethanolamine 5 that is 69.7 kcal/mol lower in energy. When the nucleophile approaches in a front-side manner as in TS-3, the longer C-O bond (0.058 Å) and N-C bond distance (0.504 Å) are reflected in a much higher activation barrier ($\Delta\Delta E^* = 14.6$ kcal/mol). The bond breaking in TS-3 is further ahead of bond making than in *anti*-TS-2. Thus, the hydrogen transfer in TS-3 affording β -hydroxyamine 5 does not occur until after the barrier is crossed, and the exothermicity of O-H bond formation and reduction in charge separation are not attainable in this sterically encumbered transition structure, further contributing to the relatively high barrier. The position of the transition structure along the reaction coordinate is clearly shown by a plot of the activation barrier versus the C-N bond distance (Figure 4).

At the other end of the reactivity spectrum we have examined the effect of a fully protonated ethylene oxide

on the barrier to amination. The O-protonated oxirane 6 is the only protonated oxirane structure that exists as a local minimum in the $\text{C}_2\text{H}_5\text{O}^+$ surface.^{12a} The protonated oxirane 6 is approximately tetrahedral at the oxygen, and inversion at the oxygen, which constrains the hydrogen in the plane (C_{2v}), has a surprisingly high barrier of 14.9 kcal/mol.^{12b} The 1-hydroxyethyl cation is predicted to be the lowest energy $\text{C}_2\text{H}_5\text{O}^+$ isomer. Rearrangement of 6 to a 1-hydroxyethyl cation (CH_3^+CHOH) is exothermic by -27.4 kcal/mol (MP2/6-31G**) in good agreement with experiment (-26 kcal/mol).¹³ Unimolecular ring opening of 6 would exhibit a high barrier since the open 2-hydroxyethyl cation ($\text{HOCH}_2\text{CH}_2^+$) resulting from C-O bond rupture lies ~24 kcal/mol higher in energy than 6. Location of a transition state for bimolecular attack of NH_3 on 6 proved to be very difficult. We found a gas-phase Cluster-7 (Figure 2) to be virtually identical in energy (Table II) to the first-order saddle point (TS-8) on the potential energy surface for formation of 2-hydroxyethyl ammonium cation 9. Thus, the descending pathway from reactants to product 9 is predicted to occur without activation from the shallow energy minimum (Cluster-7). An earlier calculation using MINDO/3 suggested that this reaction had an activation enthalpy of 13.9 kcal/mol.^{12c}

Attempts to locate a stationary point by following the reaction path (IRC)^{11c} from reactants to products at the 3-21G level were not successful. When the C-N bond distance in Cluster-7 was varied from 3.8 to 1.57 Å along the reaction pathway to 9, no stationary points could be identified. Thus, bond formation of the incoming nucleophile to the electrophilic center in 6 is significantly less than one might have anticipated. Indeed the C-N bond distance at TS-8 is elongated by 70% relative to product 9.

Our third goal was to assess the energetic consequences of catalysis by a water molecule in an effort to mimic the effect the proton donor additives have on the gel time for epoxy resin curing as noted above (Table I). The intrinsic barrier for water-assisted amination of ethylene oxide (20.7 kcal/mol) is reduced by 18.8 kcal/mol relative to TS-2 when the barrier is calculated from isolated reactants to allow a direct comparison. A reduction in the barrier of this magnitude for a single proton donor molecule would be sufficient to place the activation energy in a temperature range commensurate with industrial application. When the gas-phase barrier is calculated relative to the ethylene oxide-water cluster 10 it increases to 28.6 kcal/mol for TS-11. This transition state is much later along the

reaction coordinate than the fully protonated TS-8, and the C-N bond is only 23% longer than that in product 12. The extent of C-O bond rupture is also somewhat shorter (0.04 Å) than that in TS-2 but much further advanced than the highly exothermic process in TS-8 (0.39 Å). Formation of the final product 12 is endothermic by 19.1 kcal/mol. The global minimum would obviously be ammonium salt 9 which would be rapidly formed in a subsequent proton-transfer step. Release of the constraint on the dihedral angle ($\text{O}-\text{C}-\text{C}-\text{N} = 180^\circ$) in 9 resulted in a final $\text{O}-\text{C}-\text{C}-\text{N}$ dihedral angle of 48.5° and an 8.6 kcal/mol decrease in energy reflecting the increased hydrogen bonding. Ammonium salt 9 is weakly acidic and could also serve as an effective catalyst in this reaction. The ammonium ion (NH_4^+) lowered the barrier for amination by 22.9 kcal/mol (MINDO/3)^{12c} although proton transfer from NH_4^+ to ethylene oxide occurred synchronously with approach of the nucleophile NH_3 to the carbon atom.¹⁴ In all three anti transition structures, the ammonia does not approach the back side of the C-O bond axis with the 180° bond angle typical of an $\text{S}_\text{N}2$ displacement reaction. The N-C-O bond angle deviates significantly from 180° (18.7 – 25.1°), and the approach of the nucleophile appears to be more influenced by the ultimate bond angle (110°) in the final product (Figure 1).

In summary, a water molecule exerts a significant catalytic effect upon the rate of oxirane cleavage by the nucleophile. The trend established upon going from no proton donor, to weakly acidic water, to a fully protonated epoxide clearly establishes the mechanistic effect of additives as proton donors and their effect upon the curing rate of epoxy resins.

Acknowledgment. This work was supported in part by a grant from the National Institutes of Health (CA 47348-02) and the Ford Motor Co. We are very thankful to the Pittsburgh Supercomputing Center, the Ford Motor Co., and the Computing Center at Wayne State University for generous amounts of computing time. J.L.A. gratefully

acknowledges a fellowship from the CIRIT of the Generalitat de Catalunya (Catalonia, Spain) which has made his stay at Wayne State University possible.

References and Notes

- (1) McManus, S. P.; Larson, C. A.; Hearn, R. A. *Synth. Commun.* 1973, 3, 177.
- (2) Fieser, L. F.; Fieser, M. *Reagents for Organic Synthesis*; Wiley: New York, 1967; Vol. 1, p 796.
- (3) Parker, R. E.; Isaacs, N. S. *Chem. Rev.* 1959, 59, 737.
- (4) Schechter, L.; Wynstra, J.; Kurkijy, R. P. *Ind. Eng. Chem. Z.* 1956, 48, 94; 1957, 49, 1107.
- (5) Smith, I. T. *Polymer* 1961, 2, 95.
- (6) Isaacs, N. S.; Parker, R. E. *J. Chem. Soc.* 1960, 3497. Addy, J. K.; Laird, R. M.; Parker, R. E. *J. Chem. Soc.* 1961, 1708. Parker, R. E.; Rockett, B. W. *J. Chem. Soc. B* 1966, 681. Laird, R. M.; Parker, R. E. *J. Chem. Soc. B* 1962, 1062.
- (7) Eastham, A. M.; Darwent, B. de B.; Beaubie, P. E. *Can. J. Chem.* 1951, 29, 575.
- (8) Eastham, A. M.; Darwent, B. de B. *Can. J. Chem.* 1951, 29, 585.
- (9) Harrod, J. F. *J. Polym. Sci.* 1963, 1A, 385.
- (10) Gould, R. F. *Epoxy Resins*; Advances in Chemistry Series 92; American Chemical Society: Washington, DC, 1970.
- (11) (a) Frisch, M. J.; Head-Gordon, M.; Schlegel, H. B.; Raghavachari, K.; Binkley, J. S.; González, C.; DeFrees, D. J.; Fox, D. J.; Whiteside, R. A.; Seeger, R.; Melius, C. F.; Baker, J.; Martin, R. L.; Kahn, R. L.; Stewart, J. J. P.; Fluder, E. M.; Topiol, S.; Pople, J. A. Gaussian, Inc., Pittsburgh, PA, 1988. (b) Schlegel, H. B. *J. Comput. Chem.* 1982, 3, 214. (c) González, C.; Schlegel, H. B. *J. Chem. Phys.* 1989, 90, 2154.
- (12) (a) Ford, G. P.; Smith, C. T. *J. Am. Chem. Soc.* 1987, 109, 1325. (b) Nobes, R. H.; Rodwell, W. R.; Bauma, W. J.; Radom, L. *J. Am. Chem. Soc.* 1981, 103, 1913. (c) Shibaev, A. Y.; Astrat'eva, N. V.; Tereshchenko, G. F. *Zh. Obshch. Khim.* 1984, 54, 2744. (d) Del Bene, J. E.; Frisch, M. J.; Raghavachari, K.; Pople, J. A. *J. Phys. Chem.* 1982, 86, 1529. (e) Aue, D. H.; Webb, H. M.; Davidson, W. R. *J. Am. Chem. Soc.* 1980, 102, 5151.
- (13) Lias, S. G.; Liebman, J. F.; Levin, R. D. *J. Phys. Chem. Ref. Data* 1984, 13, 695–808.
- (14) The relative proton affinities of ammonia and ethylene oxide are -220.8 (-210.6 with ZPE)^{12d} and -190.5 kcal/mol, respectively. Experimental values are 189.6^{12e} and 205.0^{12d} kcal/mol.